6-2-2016

Method of Lines Transpose: High Order L-Stable {O}(N) Schemes for Parabolic Equations Using Successive Convolution

Matthew F. Causley

Hana Cho

Andrew J. Christlieb

David C. Seal

Method of lines transpose: High order L-stable O(N) schemes for parabolic equations using successive convolution

Article *in* SIAM Journal on Numerical Analysis · August 2015

DOI: 10.1137/15M1035094 · Source: arXiv

CITATIONS
15

READS
91

4 authors:

Matthew F Causley
Kettering University
22 PUBLICATIONS **100** CITATIONS
SEE PROFILE

Hana Cho
Michigan State University
2 PUBLICATIONS **20** CITATIONS
SEE PROFILE

Andrew Christlieb
Michigan State University
129 PUBLICATIONS **995** CITATIONS
SEE PROFILE

David Seal
United States Naval Academy
23 PUBLICATIONS **251** CITATIONS
SEE PROFILE

METHOD OF LINES TRANSPOSE: HIGH ORDER L-STABLE $\mathcal{O}(N)$ SCHEMES FOR PARABOLIC EQUATIONS USING SUCCESSIVE CONVOLUTION

MATTHEW F. CAUSLEY*, HANA CHO†, ANDREW J. CHRISTLIEB‡, AND DAVID C. SEAL§

Abstract. We present a new solver for nonlinear parabolic problems that is L-stable and achieves high order accuracy in space and time. The solver is built by first constructing a single-dimensional heat equation solver that uses fast $\mathcal{O}(N)$ convolution. This fundamental solver has arbitrary order of accuracy in space, and is based on the use of the Green's function to invert a modified Helmholtz equation. Higher orders of accuracy in time are then constructed through a novel technique known as successive convolution (or resolvent expansions). These resolvent expansions facilitate our proofs of stability and convergence, and permit us to construct schemes that have provable stiff decay. The multi-dimensional solver is built by repeated application of dimensionally split independent fundamental solvers. Finally, we solve nonlinear parabolic problems by using the integrating factor method, where we apply the basic scheme to invert linear terms (that look like a heat equation), and make use of Hermite-Birkhoff interpolants to integrate the remaining nonlinear terms. Our solver is applied to several linear and nonlinear equations including heat, Allen-Cahn, and the Fitzhugh-Nagumo system of equations in one and two dimensions.

Key words. Method of lines transpose, transverse method of lines, Rothe's method, parabolic PDEs, implicit methods, boundary integral methods, alternating direction implicit methods, ADI schemes, higher order L-stable, multiderivative

1. Introduction.

The prototypical parabolic differential equation is the heat equation. It forms a cornerstone of mathematics and physics, and its understanding is essential for defining more complicated mathematical models. Fourier introduced this equation as a means to describe transient heat flow. Fick quickly recognized its importance to particle and chemical concentrations. As a result, parabolic equations are now ubiquitous in describing diffusion processes, which are found in a vast array of physical problems, among which are reaction-diffusion models of chemical kinetics [18, 19, 34], phase field models describing morphology and pattern formation in multiphase fluids and solids [3, 4, 12], and even the volatility of stocks and bonds in mathematical finance [42].

Numerical solutions of (linear and nonlinear) diffusion equations have been the subject of active research for many decades. As early as the 1950's and 60's, it was recognized that due to the parabolic scaling, method of lines discretizations of the heat equation lead to numerically stiff systems of equations. In principal, the numerical stiffness can be subsided by taking larger time steps, which are only stable if fully implicit solvers are used. But in practice, the memory of early computers was extremely limited, making full matrix inversions difficult and costly. Thus, alternate dimensionally implicit (ADI) splitting methods [11, 13–16, 37], which utilize dimensional splitting and tridiagonal solvers, quickly gained popularity.

Later on, memory constraints no longer defined the bottleneck for computing, and attention shifted toward methods that focused on reducing floating point operations (FLOPs), albeit with additional memory constraints. Most notable among these are Krylov methods [22, 28], boundary integral methods [20, 27], and quadrature methods [23, 24, 30, 31, 44]. However, with the advent of GPU processors, it appears that we are yet again seeing a paradigm shift towards methods that should emphasize small memory footprints, even at the expense of incurring a higher operation count. Thus, ADI-like methods, which can efficiently decompose larger problems and limit overhead communication, warrant further investigation, and these features are the motivating factor for this work.

In this paper we propose a novel numerical method for obtaining solutions to the linear heat equation, and nonlinear equations of reaction-diffusion type. As an alternative to classical MOL formulations, we use the method of lines transpose (MOL^T), which is sometimes referred to as Rothe's method [38], or the transverse method of lines [39]. In this case, the PDE is discretized in time first, and the resulting semi-discrete (modified Helmholtz) problem can be solved using a variety of methods. From potential theory [22, 27], the solution can be constructed by discretizing boundary integrals. However, with dimensional splitting (that is related to the original ADI formulations), the MOL^T can be used to analytically solve simpler, one-

* Kettering University, Department of Mathematics, 1700 University Ave, Flint, Michigan, 48504, USA (mcausley@kettering.edu)

† Michigan State University, Department of Mathematics, 619 Red Cedar Rd., East Lansing, Michigan, 48824, USA (chohana@msu.edu)

‡ Michigan State University, Department of Mathematics and Electrical Engineering (andrewch@math.msu.edu)

§ U.S. Naval Academy, Department of Mathematics, 121 Blake Road, Annapolis, MD 21402, USA (seal@usna.edu)

dimensional boundary value problems, and the subsequent solution can be constructed through dimensional sweeps, resulting in an $\mathcal{O}(N \log N)$ [32, 33] or $\mathcal{O}(N)$ [5–7] solver. Furthermore, we extend the method to higher orders of accuracy by using a novel idea referred to as successive convolution. This strategy has recently been developed in [6] for the wave equation by the present authors. In the present work, we not only extend the method of lines transpose to parabolic problems, but we recognize the resulting expansion as a so-called resolvent expansion [1,21], which we leverage to prove stability and convergence of the successive convolution series. In addition, we incorporate nonlinear terms with an integrating factor method that relies on high order Hermite-Birkhoff interpolants as well as the (linear) resolvent expansions developed in this paper.

The rest of this paper is organized as follows. In Section 2 we derive the basic scheme for the one-dimensional heat equation, which is L-stable and can achieve high orders of accuracy in space and time. In Section 3 we describe how to obtain an arbitrary order discretization in a single dimension with resolvent expansions. In Section 4, we describe how this can be extended to multiple dimensions, and in Section 5 we present results for linear heat in one and two dimensions. In Section 6, we describe how our approach can handle nonlinear source terms, and in Section 7 we present numerous numerical results including Allen-Cahn and the Fitzhugh-Nagumo system of equations. Finally, we draw conclusions and point to future work in Section 8.

2. First order scheme in one spatial dimension. We begin by forming a semi-discrete solution to the 1D heat equation using the method of lines transpose (MOL^T). Let $u = u(x,t)$ satisfy

$$u_t = \gamma u_{xx}, \quad (x,t) \in (a,b) \times [0,T], \tag{2.1}$$

with constant diffusion coefficient γ, and appropriate initial and boundary conditions. The MOL^T amounts to employing a finite difference scheme for the time derivative, and collocating the Laplacian term at time levels $t = t^n$ and $t = t^{n+1}$. Following a similar to ours from [6], we introduce a free parameter $\beta > 0$, so that the collocation has the form[1]

$$\frac{u^{n+1} - u^n}{\Delta t} = \gamma \partial_{xx} \left(u^n + \frac{u^{n+1} - u^n}{\beta^2} \right), \qquad \beta > 0.$$

Next, we introduce the differential operator corresponding to the modified Helmholtz equation, defined by

$$\mathcal{L} = I - \frac{\partial_{xx}}{\alpha^2}, \quad \alpha = \frac{\beta}{\sqrt{\gamma \Delta t}}. \tag{2.2}$$

After some algebra, we find that the scheme can be written as

$$\mathcal{L}[u^{n+1} - (1-\beta^2)u^n] = \beta^2 u^n. \tag{2.3}$$

We note that there are two strategies for choosing β: first we could maximize the order, or alternatively we could enforce some important condition, such as stiff decay. Indeed, we observe that

1. If we choose $\beta^2 = 2$, then the discretization is the trapezoidal rule, which is second order accurate, A-stable, yet does not exhibit stiff decay.
2. If we choose $\beta^2 = 1$, then the discretization is the backward Euler scheme, which is first order accurate, L-stable, yet does not maximize the order of accuracy.

Here and below, we opt for the second strategy, as the stiff decay of numerical solutions of the heat equation is of paramount importance. In Section 3.2, we will develop this discussion in the context of higher order schemes that relies on a careful selection of β as well as repeated applications of a single inverse operator.

Upon solving equation (2.3) for u^{n+1}, we find that the update equation is

$$u^{n+1} = (1-\beta^2)u^n + \beta^2 \mathcal{L}^{-1}[u^n], \tag{2.4}$$

[1] In [6], there are a total of two time derivatives (and two space), so the right hand side depended on u^{n+1}, u^n, and u^{n-1}.

that requires inverting a modified Helmholtz operator. We accomplish this *analytically* by using Green's functions, from which

$$\mathcal{L}^{-1}[u] = \left(I - \frac{\partial_{xx}}{\alpha^2}\right)^{-1}[u] := \frac{\alpha}{2}\int_a^b e^{-\alpha|x-y|}u(y)dy + B_a e^{-\alpha(x-a)} + B_b e^{-\alpha(b-x)}. \tag{2.5}$$

The coefficients B_a and B_b are determined by applying prescribed boundary conditions at $x = a, b$ which we describe in Section 2.2.

REMARK 1. *Alternatively, had we followed the method of lines (MOL) and first discretized (2.1) in space, then the differential operator $\mathcal{L}$ would be replaced by an algebraic operator L, and would be inverted numerically.*

REMARK 2. *Although the update (2.4) (with $\beta \neq 1$), is only first order accurate, we describe in Section 3 how to extend our procedure to arbitrary order in time.*

This MOL^T approach has several advantages. First, the solution is now explicit, but remains unconditionally stable. Secondly, in recent work [5–7] we show that the convolution integral in Eqn. (2.5) can be discretized using a fast $\mathcal{O}(N)$ algorithm, where N is the number of spatial points. We introduce more details in Section 2.1, wherein we update the current algorithm to achieve a user-defined accuracy of $\mathcal{O}(\Delta x^M)$ with mesh spacing Δx. Finally, since the solution is still continuous in space, we can decouple the spatial and temporal errors, and by combining resolvent expansions with dimensional splitting, we extend the method to multiple dimensions without recoupling the errors.

REMARK 3. *Since dimensional splitting is used, all spatial quantities are computed according to a one-dimensional convolution integral of the form (2.5), which is performed on a line-by-line basis, following so-called "dimensional sweeps". Since the discrete convolution is computed in $\mathcal{O}(N)$ complexity, the full solver scales linearly in the number of spatial points (assuming each sweep is performed in parallel).*

A fully discrete scheme is obtained after a spatial discretization of (2.5). The domain $[a, b]$ is partitioned into N subdomains $[x_{j-1}, x_j]$, with $a = x_0 < x_1 < \ldots x_N = b$. The convolution operator is comprised of a particular solution, which is defined by the convolution integral

$$I[u](x) := \frac{\alpha}{2}\int_a^b e^{-\alpha|x-y|}u(y)dy \tag{2.6}$$

and a homogeneous solution

$$B_a e^{-\alpha(x-a)} + B_b e^{-\alpha(b-x)}, \tag{2.7}$$

both of which can be constructed in $\mathcal{O}(N)$ operations using fast convolution. We now describe each of these in turn, starting with the first.

2.1. Spatial discretization of the particular solution. The particular solution is first split into $I[u](x) = I^L(x) + I^R(x)$, where

$$I^L(x) = \frac{\alpha}{2}\int_a^x e^{-\alpha(x-y)}u(y)dy, \quad I^R(x) = \frac{\alpha}{2}\int_x^b e^{-\alpha(y-x)}u(y)dy.$$

Each of these parts independently satisfy the first order "initial value problems"

$$\begin{aligned}(I^L)'(y) + \alpha I^L(y) &= \frac{\alpha}{2}u(y), \quad a < y < x, \quad I^L(a) = 0,\\ (I^R)'(y) - \alpha I^R(y) &= -\frac{\alpha}{2}u(y), \quad x < y < b, \quad I^R(b) = 0,\end{aligned}$$

where the prime denotes spatial differentiation. By symmetry, the scheme for I^R follows from that of I^L, which we describe. From the integrating factor method, the integral satisfies the following identity, known as exponential recursion

$$I^L(x_j) = e^{-\nu_j} I^L(x_{j-1}) + J^L(x_j), \quad \text{where} \quad J^L(x_j) = \frac{\alpha}{2}\int_{x_{j-1}}^{x_j} e^{-\alpha(x_j-y)}u(y)dy,$$

and

$$\nu_j = \alpha h_j, \qquad h_j = x_j - x_{j-1}.$$

This expression is still exact, and indicates that only the "local" integral J^L needs to be approximated. We therefore consider a projection of $u(y)$ onto P_M, the space of polynomials of degree M. A local approximation

$$u(x_j - zh_j) \approx p_j(z), \quad z \in [0,1],$$

will be accurate to $\mathcal{O}(h_j^M)$, and defines a quadrature of the form

$$J^L(x_j) = \frac{\nu_j}{2}\int_0^1 e^{-\nu_j z} u(x_j - h_j z)dz \approx \frac{\nu_j}{2}\int_0^1 e^{-\nu_j z} p_j(z)dz. \tag{2.8}$$

If standard Lagrange interpolation is used, then the polynomials can be factorized as

$$p_j(z) = \sum_{k=-\ell}^{r} p_{jk}(z) u_{j+k} = z^T A_j^{-1} u_j^M, \tag{2.9}$$

where $z = [1, z, \ldots, z^M]^T$, and $u_j^M = [u_{j-\ell}, \ldots, u_j, \ldots, u_{j+r}]^T$, and A_j is the Vandermonde matrix corresponding to the points x_{j+k}, for $k = -\ell \ldots r$. The values of ℓ and r are such that $\ell + r = M + 1$, and are centered about j except near the boundaries, where a one-sided stencil is required.

Substitution of this factorization into (2.8) and integrating against the exponential, we find that

$$J^L(x_j) \approx J_j^L := \sum_{k=-\ell}^{r} w_{jk} u_{j+k},$$

where the weights $w_j = [w_{j,-\ell}, \ldots w_{j,r}]$ satisfy

$$w_j^T = \phi_j^T A_j^{-1} \tag{2.10}$$

and where

$$\phi_{jk} = \frac{\nu_j}{2}\int_0^1 e^{-\nu_j z} z^k dz = \frac{k! e^{-\nu_j}}{2\nu_j}\left(e^{\nu_j} - \sum_{p=0}^{k}\frac{(\nu_j)^p}{p!}\right).$$

If the weights are pre-computed, then the fast convolution algorithm scales as $\mathcal{O}(MN)$ per time step, and achieves a user-defined order M in space. In every example shown in this work, we choose $M = 2$ or $M = 4$.

2.2. Homogeneous solution. The homogeneous solution in (2.7) is used to enforce boundary conditions. We first observe that all dependence on x in the convolution integral, $I[x] := I[u^n](x)$ in (2.6) is on the Green's function, which is a simple exponential function. Through direct differentiation, we obtain

$$I_x(a) = \alpha I(a), \quad I_x(b) = -\alpha I(b). \tag{2.11}$$

Various boundary conditions at $x = a$ and $x = b$ can be enforced by solving a simple 2×2 system for the unknowns B_a and B_b. For example, for periodic boundary conditions we assume that (at each discrete time step, $t = t^n$)

$$u^n(a) = u^n(b), \quad u_x^n(a) = u_x^n(b), \qquad \forall n \in \mathbb{N}. \tag{2.12}$$

We next enforce this assumption to hold on the scheme (2.5),

$$\begin{aligned}
\mathcal{L}^{-1}[u^n](a) = \mathcal{L}^{-1}[u^n](b) \quad &\Longleftrightarrow \quad I(a) + B_a + B_b\mu = I(b) + B_a\mu + B_b, \\
\mathcal{L}_x^{-1}[u^n](a) = \mathcal{L}_x^{-1}[u^n](b) \quad &\Longleftrightarrow \quad \alpha\left(I(a) - B_a + B_b\mu\right) = \alpha\left(-I(b) - B_a\mu + B_b\right),
\end{aligned}$$

where $\mu = e^{-\alpha(b-a)}$ and the identities (2.11) are used to find $\mathcal{L}_x^{-1}$. Solving this linear system yields

$$B_a = \frac{I(b)}{1-\mu}, \quad B_b = \frac{I(a)}{1-\mu}. \tag{2.13}$$

Different boundary conditions (e.g. Neumann) follow an analogous procedure that requires solving a simple 2×2 linear system for B_a and B_b.

3. Higher order schemes from resolvent expansions. In our recent work [6], we apply a successive convolution approach to derive high order A-stable solvers for the wave equation. The key idea is to recognize the fact that, in view of the modified Helmholtz operator (2.2), the second derivative can be factored as

$$\left(-\frac{\partial_{xx}}{\alpha^2}\right) = \mathcal{L} - I = \mathcal{L}\left(I - \mathcal{L}^{-1}\right) := \mathcal{L}\mathcal{D}, \tag{3.1}$$

where

$$\mathcal{D} = I - \mathcal{L}^{-1}, \qquad \mathcal{L} = (I - \mathcal{D})^{-1}. \tag{3.2}$$

Substitution of the second expression into (3.1) determines the second derivative completely in terms of this new operator

$$\left(-\frac{\partial_{xx}}{\alpha^2}\right) = (I - \mathcal{D})^{-1}\,\mathcal{D} = \sum_{p=0}^{\infty} \mathcal{D}^p. \tag{3.3}$$

This shows that second order partial derivatives of a sufficiently smooth function $u(x)$ can be approximated by truncating a resolvent expansion based on successively applying $\mathcal{D}$ to $u(x)$, which is a linear combination of successive convolutions (2.5).

Now, we consider a solution $u(x,t)$ to the heat equation (2.1), that for simplicity we take to be infinitely smooth. We perform a Taylor expansion on $u(x, t+\Delta t)$, and then use the Cauchy-Kovalevskaya procedure [9, 40] to exchange temporal and spatial derivatives to yield

$$u(x,t+\Delta t) = \sum_{p=0}^{\infty} \frac{(\Delta t \partial_t)^p}{p!} u(x,t) = \sum_{p=0}^{\infty} \frac{(\gamma \Delta t \partial_{xx})^p}{p!} u(x,t) =: e^{\gamma \Delta t \partial_{xx}} u(x,t). \tag{3.4}$$

The term $e^{\gamma \Delta t \partial_{xx}}$ is a spatial pseudo-differential operator, and it compactly expresses the full Taylor series. Our goal is to make use of the formula (3.3) to convert the Taylor series into a resolvent expansion. This can be performed term-by-term, and requires rearranging a doubly infinite sum. However, if instead we work directly with the operator defining the Taylor series, then

$$e^{\gamma \Delta t \partial_{xx}} = e^{-\beta^2\left(-\frac{\partial_{xx}}{\alpha^2}\right)} = e^{-\beta^2 (I-\mathcal{D})^{-1}\mathcal{D}}.$$

At first glance this expression looks quite unwieldy. However, fortune is on our side, since the generating function of the *generalized Laguerre* polynomials $L_p^{(\lambda)}(z)$ is

$$\sum_{p=0}^{\infty} L_p^{(\lambda)}(z) t^p = \frac{1}{(1-t)^{\lambda+1}} e^{-\frac{tz}{1-t}}, \tag{3.5}$$

which bears a striking resemblance to our expansion. Indeed, if we take $\lambda = -1$, substitute $z = \beta^2$ and $t = \mathcal{D}$, then

$$e^{-\beta^2 (I-\mathcal{D})^{-1}\mathcal{D}} = \sum_{p=0}^{\infty} L_p^{(-1)}(\beta^2) D^p = I + \sum_{p=1}^{\infty} L_p^{(-1)}(\beta^2) D^p. \tag{3.6}$$

3.1. Convergence. This expansion has been considered in the context of C_0- semigroups [1,21], where $\left(-\frac{\partial_{xx}}{\alpha^2}\right)$ is replaced with a general closed operator A on a Hilbert space X. In our notation, we restate part (ii) of Theorem 4.3 in [1], which is proven therein.

THEOREM 3.1. *Let the C_0- semigroup*

$$T(\beta^2) = e^{-\beta^2\left(-\frac{\partial_{xx}}{\alpha^2}\right)} = \sum_{p=0}^{\infty} L_p^{(-1)}(\beta^2) \left(I - \frac{\partial_{xx}}{\alpha^2}\right)^{-p} \left(-\frac{\partial_{xx}}{\alpha^2}\right)^p$$

$$= \sum_{p=0}^{\infty} L_p^{(-1)}(\beta^2) \mathcal{L}^{-p} (\mathcal{L} - I)^p = \sum_{p=0}^{\infty} L_p^{(-1)}(\beta^2) D^p$$

be approximated by

$$T_P(\beta^2) = \sum_{p=0}^{P} L_p^{(-1)}(\beta^2) D^p.$$

Then, for $u(x) \in C^{2P+2}$, there exists for each $\beta^2 > 0$ an integer m_0 such that for all integers $2 \le k \le P+1$, with $P \ge m_0$,

$$\left\| T(\beta^2)u - T_P(\beta^2)u \right\| \le \frac{C(\beta^2, k)}{P^{k/2-1}} \left\| \left(-\frac{\partial_{xx}}{\alpha^2} \right)^k u \right\|,$$

where $C(\beta^2, k)$ is a constant that depends only on β^2 and k.

REMARK 4. *The salient point of the theorem is that, in consideration of α (c.f. Eqn. (2.2)), the approximation error is of the form $C\Delta t^{P+1} \left\| u^{(2P+2)}(x) \right\|$, which matches the form given by a typical Taylor method.*

We now truncate the resolvent expansion (3.6) at order $p = P$, and find that for the heat equation,

$$u(x, t+\Delta t) = u(x,t) + \sum_{p=1}^{P} L_p^{(-1)}(\beta^2) \mathcal{D}^p[u](x,t), \tag{3.7}$$

has a truncation error of the form

$$\tau := L_{P+1}^{(-1)}(\beta^2) \mathcal{D}^{P+1}[u](x,t) + \mathcal{O}(\Delta t^{P+2}). \tag{3.8}$$

The first few schemes, evaluated at $t = t^n$ are

$$u^{n+1} = u^n - \beta^2 \mathcal{D}[u^n], \tag{3.9}$$

$$u^{n+1} = u^n - \beta^2 \mathcal{D}[u^n] - \left(\beta^2 - \frac{\beta^4}{2} \right) \mathcal{D}^2[u^n], \tag{3.10}$$

$$u^{n+1} = u^n - \beta^2 \mathcal{D}[u^n] - \left(\beta^2 - \frac{\beta^4}{2} \right) \mathcal{D}^2[u^n] - \left(\beta^2 - \beta^4 + \frac{\beta^6}{6} \right) \mathcal{D}^3[u^n]. \tag{3.11}$$

We note that for implementation, each operator is applied successively, and is defined by

$$\mathcal{D}^{(p+1)}[u] := \mathcal{D}[\mathcal{D}^p[u]], \quad \mathcal{D}^0[u] := u.$$

3.2. Stability. There remains one critical issue: the choice of the free parameter β. In 1974, Nørsett studied a similar single-step multiderivative method for the heat equation [35] and he too, had a free parameter in his solver. We follow his lead on the Von-Neumann analysis based on his MOL discretization, but in this work we optimize β to obtain stiff decay, whereas Nørsett chose β to maximize the order of accuracy of the solver.

Consider the linear test problem

$$\frac{dy}{dt} = \lambda y, \qquad y(0) = 1, \quad \lambda \in \mathbb{C},$$

whose exact solution $y(t)$ satisfies

$$y(t+h) = e^z y(t), \quad z = h\lambda \in \mathbb{C}.$$

Application of (3.7) to this test problem results in

$$y(t+h) = \sum_{p=0}^{P} L_p^{(-1)}(\beta^2) \hat{D}^p y(t) = \phi(z) y(t)$$

where

$$\hat{D} = \frac{-(z/\beta^2)}{1-(z/\beta^2)} = 1 - \left(1-(z/\beta^2)\right)^{-1}.$$

The generalized Laguerre polynomials satisfy many identities, the following of which is the most pertinent:

$$L_{p+1}^{(0)}(x) - L_p^{(0)}(x) = L_{p+1}^{(-1)}(x) = \left(\frac{x}{p+1}\right)\frac{d}{dx}L_{p+1}^{(0)}(x). \tag{3.12}$$

Here, $L_p^{(0)}(x)$ is the standard Laguerre polynomial $L_p(x)$. Following standard definitions, we say that a numerical scheme is *A-stable*, provided $|\phi| \leq 1$ in the left-half of the complex plane $z \in \mathbb{C}^-$. Likewise, a scheme exhibits *stiff decay* if $\phi(z) \to 0$ as $Re(z) \to -\infty$. If an A-stable method also exhibits stiff decay, it is L-stable.

Now, observing that $\hat{D} \to 1$ as $Re(z) \to -\infty$, we find that

$$\lim_{z\to-\infty}\phi(z) = \sum_{p=0}^{P} L_p^{(-1)}(\beta^2) = L_0^0(\beta^2) + \sum_{p=1}^{P}\left(L_p^0(\beta^2) - L_{p-1}^0(\beta^2)\right) = L_P^0(\beta^2), \tag{3.13}$$

where we have used the first two expressions in (3.12) to introduce a telescoping sum. We are now prepared to prove the following

THEOREM 3.2. *Let $u(x,t)$ be an approximates solution to the heat equation (2.1), given by the successive convolution scheme (3.7). Then,*

1. *If $\beta^2 = x_1^{(P)}$ is chosen as the smallest root of $L'_{P+1}(x) = (L_{P+1}^{(0)}(x))'$, then the scheme achieves order $P+1$, but does not exhibit stiff decay.*
2. *If $\beta^2 = x_1^{(P)}$ is chosen as the smallest root of $L_P(x) = L_P^{(0)}(x)$, then the scheme achieves order P, and exhibits stiff decay.*
3. *Following the first strategy, the schemes are A-stable for $P = 1, 2, 3$, whereas the second strategy ensures L-stability. For both strategies, $A(\alpha)$-stability is achieved for $P > 3$, with large values of $\alpha \approx \pi/2$.*

Proof. The proof follows by applying the maximum modulus principle coupled with (3.13). For part 1, upon examining the truncation error (3.8), we see that an additional order of accuracy can be gained if we choose

$$L_{P+1}^{(-1)}(\beta^2) = \left(\frac{\beta^2}{P+1}\right)L'_{P+1}(\beta^2) = 0.$$

However, $L_P(\beta^2) \neq 0$ for this choice, and so stiff decay does not hold. For part 2, we instead enforce stiff decay, but then the truncation error is of order P. Finally, part 3 is demonstrated by the maximum amplification factors ϕ along the imaginary axis, as shown for both strategies in Figure 1. In particular, we observe that $|\phi(iy)| \leq 1$ for $P = 1, 2, 3$. ∎

REMARK 5. *In [35], the scheme was chosen to maximize the order of accuracy, implicitly leading to eliminating the first term in the truncation error (3.8), which is equivalent to the first strategy. However, in this work we follow the second strategy, and choose β^2 as the smallest root of $L_P(x)$ to ensure stiff decay.*

For comparison we record the values of β^2 chosen for each order $1 \leq P \leq 6$, to those of Nørsett in Table 1. For all of our solvers, we choose β to be the largest possible value that still yields provable stiff decay.

4. Resolvent expansions for multiple spatial dimensions. We extend the 1D solver to multiple spatial dimensions through the use of dimensional splitting. Our key observation is that we can use the factorization property of the exponential to perform the series expansion. For instance, in three dimensions, we have

$$e^{\gamma\Delta t\nabla^2} = e^{-\beta^2\left(-\frac{\partial_{xx}}{\alpha^2}\right)}e^{-\beta^2\left(-\frac{\partial_{yy}}{\alpha^2}\right)}e^{-\beta^2\left(-\frac{\partial_{zz}}{\alpha^2}\right)}. \tag{4.1}$$

Now, we first replace each term with the identity (3.6) dimension by dimension, and then truncate the expansions which will be in terms of the univariate operators $\mathcal{L}_\gamma^{-1}$ and $\mathcal{D}_\gamma$ for $\gamma = \{x, y, z\}$ as defined by

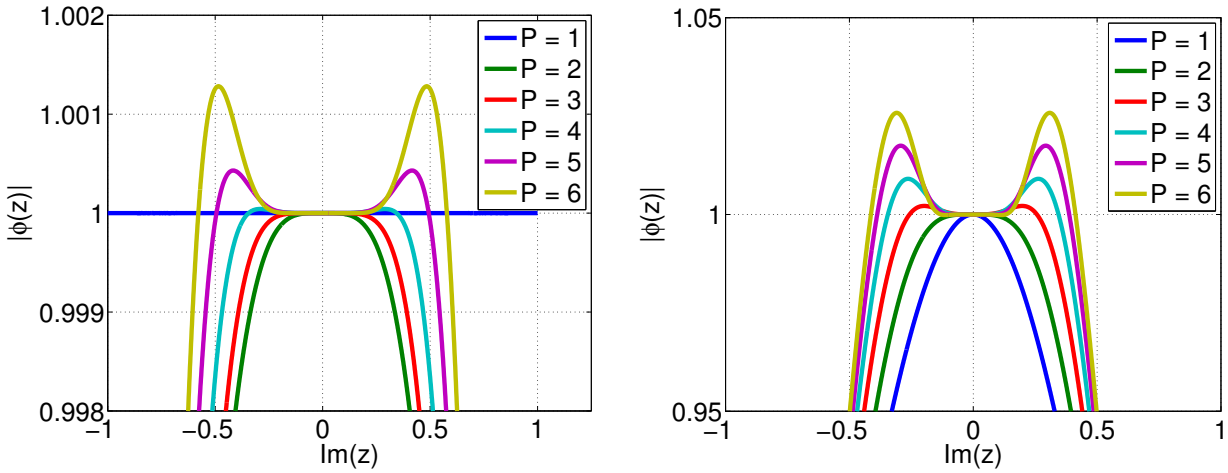

(a) Maximal Order (b) Stiff Decay

Fig. 1: Maximum amplification factors $|\phi(iy)|$ for the first few orders P, with (a) maximal order, or (b) stiff decay. When maximizing order, the first 3 schemes exhibit A-stability, whereas ensuring stiff decay leads to L-stable schemes. For $P > 3$, both schemes become $A(\alpha)$-stable.

Table 1: Values of β^2 chosen for orders $P = 1, 2, \ldots 6$. The first column are those used in our schemes, and uniquely guarantee stiff decay and $A(0)$-stability. For comparison, we also display the values in Nørsett [35] which give optimal order $P + 1$, at the expense of stiff decay.

	Stiff Decay		Maximal Order	
P	β^2	$L_P(\beta^2)$	β^2	$L_P(\beta^2)$
1	1.0000	0	2.0000	-1.0000
2	0.5858	0	1.2679	-0.7320
3	0.4158	0	0.9358	-0.6304
4	0.3225	0	0.7433	-0.5768
5	0.2636	0	0.6170	-0.5436
6	0.2228	0	0.5277	-0.5211

(2.2), and (3.7) acting on a function $u^n(x, y, z)$. This infinite sum with three indices must then be truncated to order P, and after a change of indices we find

$$E_P = \sum_{p,q,r} \binom{P-1}{p,q,r} L_p^{(-1)}(\beta^2) L_q^{(-1)}(\beta^2) L_r^{(-1)}(\beta^2) \mathcal{D}_x^p \mathcal{D}_y^q \mathcal{D}_z^r, \tag{4.2}$$

in 3D, with the corresponding 2D operator given by

$$E_P = \sum_{p,q} \binom{P-1}{p,q} L_p^{(-1)}(\beta^2) L_q^{(-1)}(\beta^2) \mathcal{D}_x^p \mathcal{D}_y^q. \tag{4.3}$$

Here we adopt the notation that sums are taken over all non-negative indices that sum to P, and the multinomial coefficients are defined such that $\binom{n}{p,q,r} = \frac{n!}{p!q!r!}$ and $\binom{n}{p,q} = \frac{n!}{p!q!}$.

REMARK 6. *The proof of stability for the multi-dimensional algorithm follows directly from that of the one-dimensional case, with the same approach applied to each spatial dimension (i.e. $\phi(z) = \phi_x(z)\phi_y(z)$ for the 2D case, and similarly for the 3D case).*

5. The heat equation.

5.1. Heat equation in 1D. We first illustrate the accuracy of our method for the 1D heat equation defined in (2.1). We consider initial conditions $u(x,0) = \sin(x)$, for $x \in [0, 2\pi]$ with periodic boundary conditions. We integrate up to a final time of $T = 4$, and set $\gamma = 0.18^2$. We use the fast convolution algorithm that is fourth order accurate in space ($M = 4$), and set the spatial grid size to be $\Delta x = \frac{2\pi}{1024} \approx 0.0061$. This ensures that the dominant error in the solution is temporal. We compute errors by the L^∞-norm, and compare against the exact solution $u(x,T) = e^{-\gamma T} u_0(x)$ at $T = 4$. The result of a temporal refinement study for $P = 1, 2$ and 3 is presented in Table 2.

Table 2: Refinement study for a 1D Heat equation defined in 5.1.

	$P=1$		$P=2$		$P=3$	
Δt	L^∞ error	order	L^∞ error	order	L^∞ error	order
0.1	1.8405×10^{-4}	–	1.6255×10^{-6}	–	2.4225×10^{-8}	–
0.05	9.2121×10^{-5}	0.9985	4.0841×10^{-7}	1.9928	3.0620×10^{-9}	2.9839
0.025	4.6084×10^{-5}	0.9993	1.0236×10^{-7}	1.9964	3.8501×10^{-10}	2.9915
0.0125	2.3048×10^{-5}	0.9996	2.5622×10^{-8}	1.9982	4.8402×10^{-11}	2.9918
0.00625	1.1525×10^{-5}	0.9998	6.4097×10^{-9}	1.9990	6.2021×10^{-12}	2.9642

5.2. Heat equation in 2D. As a second example, we present results for the 2D heat equation. We consider initial conditions $u(x,y,0) = \sin(x)\sin(y)$, for $(x,y) \in [0, 2\pi] \times [0, 2\pi]$ with periodic boundary conditions. We use a uniform mesh of size $\Delta x = \Delta y = 2\pi/512 \approx 0.0123$. Likewise, the L^∞-error is computed by comparing against the exact solution $u(x,y,T) = e^{-2\gamma T} u_0(x,y)$ at the final time $T = 1$. In Table 3, we present results for a temporal refinement study for orders $P = 1, 2$, and 3.

Table 3: Refinement study for a 2D Heat equation defined in 5.2.

	$P=1$		$P=2$		$P=3$	
Δt	L^∞-error	order	L^∞-error	order	L^∞-error	order
0.1	9.8182×10^{-5}	–	8.6717×10^{-7}	–	1.2925×10^{-8}	–
0.05	4.9143×10^{-5}	0.9985	2.1788×10^{-7}	1.9928	1.6354×10^{-9}	2.9825
0.025	2.4584×10^{-5}	0.9992	5.4608×10^{-8}	1.9963	2.0791×10^{-10}	2.9756
0.0125	1.2295×10^{-5}	0.9996	1.3672×10^{-8}	1.9979	2.9204×10^{-11}	2.8317

6. Reaction-diffusion systems. We next extend our method to nonlinear reaction-diffusion system of the form

$$\mathbf{u}_t = \mathbf{D}\nabla^2 \mathbf{u} + \mathbf{F}(\mathbf{u}), \quad (\mathbf{x}, t) \in \Omega \times (0, T], \tag{6.1}$$

where $\mathbf{u} = (u_1, u_2, \cdots, u_N)$ with $u_i = u_i(\mathbf{x}, t)$, $\mathbf{D}$ is diffusion coefficient matrix, and reaction term $\mathbf{F} := (f_1, f_2, \cdots, f_N)$ is dependent on u_i, $(i = 1, 2, \cdots, N)$. In the above, $\Omega \subset \mathbb{R}^N$ is a bounded domain with appropriate initial and boundary conditions. We shall view the diffusion as being the linear part of the differential operator, and invert this linear part analytically. Using operator calculus, we apply the integrating factor method and observe

$$\left(\partial_t - \mathbf{D}\nabla^2\right)\mathbf{u} = \mathbf{F} \quad \Longrightarrow \quad \left(e^{-\mathbf{D}t\nabla^2}\mathbf{u}\right)_t = e^{-\mathbf{D}t\nabla^2}\mathbf{F}, \tag{6.2}$$

where $e^{-\mathbf{D}t\nabla^2}$ is a diagonal matrix which composed of resolvent expansions. Equation (6.2) can now be integrated over the interval $[t, t+\Delta t]$, resulting in an exact update

$$\begin{aligned}\mathbf{u}(t+\Delta t) - e^{\mathbf{D}\Delta t\nabla^2}\mathbf{u}(t) &= \int_t^{t+\Delta t} e^{\mathbf{D}(t+\Delta t-\tau)\nabla^2}\mathbf{F}(\tau)d\tau \\ &= \int_0^{\Delta t} e^{\mathbf{D}(\Delta t-\tau)\nabla^2}\mathbf{F}(t+\tau)d\tau,\end{aligned} \tag{6.3}$$

where we have made use of the abbreviated notation, $\mathbf{F}(t) := \mathbf{F}(\mathbf{u}(\mathbf{x}, t))$. We integrate the linear part of the equation to high order using resolvent expansion based on the successive convolution operators described thus far. The additional difficulty here is the inclusion of the nonlinear reaction term, to which we propose handling in the following manner.

Our most straightforward approach results in a second order implicit scheme that is obtained by approximating (6.3) with the trapezoidal integration rule. This defines

$$\mathbf{u}(t+\Delta t) - e^{\mathbf{D}\Delta t\nabla^2}\mathbf{u}(t) = \frac{\Delta t}{2}\left[e^{\mathbf{D}\Delta t\nabla^2}\mathbf{F}(t) + \mathbf{F}(t+\Delta t)\right], \tag{6.4}$$

as a single step update. In order to obtain higher order accuracy, we propose discretizing the integrand in (6.3) with a third order Hermite-Birkhoff interpolant and performing exact integration of the resulting function to yield the third order scheme

$$\mathbf{u}(t+\Delta t) - e^{\mathbf{D}\Delta t\nabla^2}\mathbf{u}(t) = e^{\mathbf{D}\Delta t\nabla^2}\left[\frac{2\Delta t}{3}\mathbf{F}(t) + \frac{\Delta t}{6}\left(-\mathbf{D}\Delta t\nabla^2\mathbf{F}(t) + \Delta t\frac{d\mathbf{F}}{d\mathbf{t}}(t)\right)\right] + \frac{\Delta t}{3}\mathbf{F}(t+\Delta t), \tag{6.5}$$

where $\frac{d\mathbf{F}}{dt}(t) = \frac{d\mathbf{F}}{d\mathbf{u}}(t)\cdot(\mathbf{D}\nabla^2\mathbf{u}(t) + \mathbf{F}(t))$. The Hermite-Birkhoff interpolant that matches the integrand in (6.3) at times $\tau = 0$, and $\tau = \Delta t$, as well as its derivative at time $\tau = 0$ produces the quadrature rule in (6.5).

REMARK 7. *The proposed schemes in* (6.4) *and* (6.5) *produce nonlinear equations for* $\mathbf{u}(x, t+\Delta t)$ *that need to be solved at each time step. Therefore, any implicit solver will necessarily be problem dependent.*

For the problems examined in this work, we make use of simple fixed-point iterative schemes. We stabilize our iterative solvers by linearizing $\mathbf{F}(\mathbf{u})$ about a background state $\mathbf{F}_\mathbf{u}(\mathbf{u}^*)$, which depends on the problem under consideration.

6.1. A discretization of the Laplacian operator. It remains to define a numerical discretization of the Laplacian operator ∇^2 that shows up in (6.5). Following the expansion of the one-dimensional operator (3.3), we observe that

$$-\frac{\nabla^2}{\alpha^2} = -\frac{\partial_{xx}}{\alpha^2} - \frac{\partial_{yy}}{\alpha^2} = \sum_{p=1}^{\infty}\left(\mathcal{D}_x^p + \mathcal{D}_y^p\right),$$

still holds, and can be truncated at the appropriate accuracy $p = P$. Here, the subscripts indicate that the convolution is only in one spatial direction, and the other variable is held fixed. Thus, $\mathcal{D}_x$ is applied along horizontal lines for fixed y-values, and likewise for $\mathcal{D}_y$.

7. Nonlinear numerical results.

7.1. Allen-Cahn. We examine in greater detail of our schemes for the Allen-Cahn (AC) equation [2],

$$u_t = \epsilon^2\nabla^2 u + f(u), \qquad (x,t)\in\Omega\times(0,T], \tag{7.1}$$

where the reaction term is $f(u) = u - u^3$, and $\Omega\subset\mathbb{R}^d$ is a bounded domain, and u satisfies homogeneous Neumann boundary conditions.

For our fixed point iteration, we linearize f about the stable fixed points $u^* = \pm 1$, which satisfy $f'(u^*) = 0$. For example, the second order scheme from (6.4) becomes

$$(1+\Delta t)\,u^{n+1,k+1} = e^{\epsilon^2\Delta t\nabla^2}\left(u^n + \frac{\Delta t}{2}f^n\right) + \frac{\Delta t}{2}\left(f^{n+1,k} + 2u^{n+1,k}\right), \tag{7.2}$$

where k is an index that defines an iteration number. Likewise, the third order scheme from (6.5) becomes

$$\left(1+\frac{2\Delta t}{3}\right)u^{n+1,k+1} = e^{\epsilon^2\Delta t\nabla^2}\left[u^n+\frac{2\Delta t}{3}f^n+\frac{\Delta t}{6}\left(-\epsilon^2\Delta t\nabla^2 f^n+\Delta t f_t^n\right)\right]+\frac{\Delta t}{3}\left(f^{n+1,k}+2u^{n+1,k}\right). \tag{7.3}$$

Here, $e^{\epsilon^2\Delta t\nabla^2}$ is again understood by replacing it with a resolvent expansion, which is a truncated series of successive convolution operators.

7.2. Allen-Cahn: One-dimensional test. In order to see the accuracy of our proposed scheme, we calculate equilibrium profiles of for a well-known traveling solution [8, 29],

$$u_{AC}(x,t) = \frac{1}{2}\left(1-\tanh\left(\frac{x-T_s-st}{2\sqrt{2}\epsilon}\right)\right), \qquad x\in\Omega=[0,4], \quad 0\le t\le T. \tag{7.4}$$

Here, $s=\frac{3\epsilon}{\sqrt{2}}=0.09$ is the speed of the traveling wave, and we choose $\epsilon=0.03\sqrt{2}$. Additionally, we choose $T_s := 1.5-sT$ so that the exact solution satisfies $u_{AC}(1.5,T)=0.5$ for any time step size.

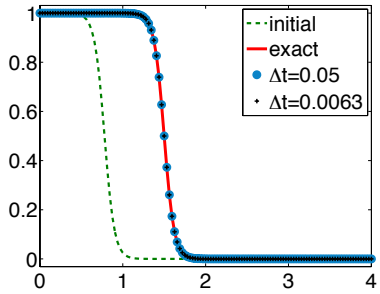

Fig. 2: Traveling wave solutions $u(x,T)$ at $T=8$ from our scheme (7.2) with two different time step sizes, compared with the exact profile in (7.4).

Results of our solver for a final time of $T=8$ are shown in Figure 2. We use a fixed spatial mesh $\Delta x = 2^{-6}\approx 0.0156$, and time steps of size $\Delta t = 0.05$ and $\Delta t = 0.00625$. This simulation shows that even with the larger Δt, the traveling solution obtained from our proposed method travels with a correct speed, as we expect.

Table 4: Refinement study for the 1D Allen-Cahn (AC) with a known exact solution as described in 7.2.

	$P=1$		$P=2$		$P=3$	
Δt	L^∞ error	order	L^∞ error	order	L^∞ error	order
0.025	2.8216×10^{-4}	–	1.3895×10^{-5}	–	2.6060×10^{-6}	–
0.0125	1.4419×10^{-4}	0.9686	3.6115×10^{-6}	1.9439	3.9417×10^{-7}	2.7249
0.0063	7.2874×10^{-5}	0.9845	9.2164×10^{-7}	1.9703	5.5010×10^{-8}	2.8411
0.0031	3.6632×10^{-5}	0.9923	2.3294×10^{-7}	1.9842	7.3122×10^{-9}	2.9113
0.0016	1.8365×10^{-5}	0.9961	5.8695×10^{-8}	1.9886	9.5714×10^{-10}	2.9335

To show the accuracy of our schemes, we check the L^∞-error using the exact solution $u_{AC}(x,T)$ (7.4) at a final time of $T=1$. In Table 4, we observe the first and second order accuracy in time from the second order scheme (7.2) and the third order from (7.3). Again, we use the fourth order spatial scheme with fixed mesh $\Delta x = 2^{-9}$ to ensure that the dominant error is temporal. Our scheme can achieve higher order accuracy in space, as well as in time, which would require using higher order Hermite interpolation of the temporal integral in (6.3).

7.3. Allen-Cahn: Two-dimensional test. In this section, we apply our proposed scheme to a two-dimensional problem with the homogeneous Neumann boundary conditions. We use a standard benchmark problem in two-dimensions that describes the motion of circular interface [8,29,41], to which a limiting exact solution is known. The radially symmetric initial conditions are defined by

$$u(x,y,0) = \tanh\left(\frac{0.25 - \sqrt{(x-0.5)^2 + (y-0.5)^2}}{\sqrt{2}\epsilon}\right), \tag{7.5}$$

which has the interfacial circle ($u(x,y,0) = 0$) centered at $(0.5, 0.5)$ with a radius of $R_0 = 0.25$. Such a interfacial circle is unstable, and thus the circle will shrink by the rate of the mean curvature [2]

$$V = \frac{dR}{dt} = -\frac{1}{R}, \tag{7.6}$$

where V is the velocity of the moving interface, and R is the radius of the interfacial circle at t ($u(x,y,t) = 0$). The negative sign indicates the interface moves towards its center of curvature. By integrating (7.6) with respect to time, we have

$$R(t) = \sqrt{R_0^2 - 2\epsilon^2 t}. \tag{7.7}$$

Due to the scaling of our diffusion coefficient, we note that our definition of (7.1) has a different, but equivalent time scale than that of [8,29,41].

We simulate the time evolution of $u(x,y,0)$ in (7.5) using the proposed second order scheme (fourth order in space) where we use the same parameters as [29], but rescale with $\epsilon = 0.05$, $\Delta t = \frac{6.4\times 10^{-4}}{\epsilon^2} = 0.0256$, and $\Delta x = \Delta y = 2^{-8} \approx 0.0039$. In Figure 3, we observe that the interfacial circle shrinks, as is expected.

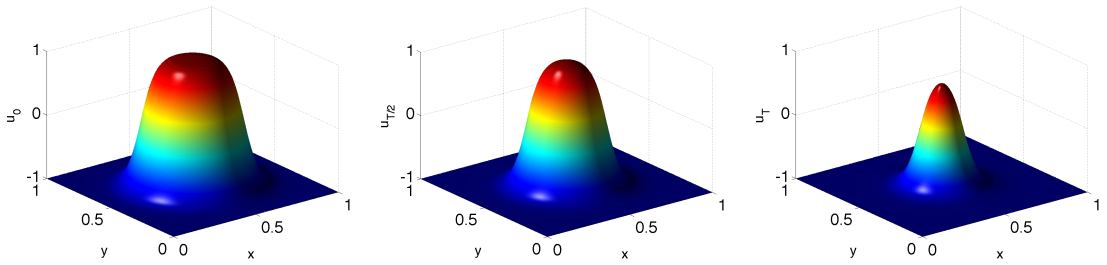

(a) $u(x,y,0)$ (b) $u(x,y,\frac{T}{2})$ (c) $u(x,y,T)$

Fig. 3: Time evolution of (7.5) using our scheme at $0 \le t \le T = \frac{0.0256}{\epsilon^2} = 10.24$.

Next, we verify that our numerical schemes calculate the accurate velocity of this moving circle problem. In Figure 4, we plot the evolution of the radii obtained by our second order scheme with the two different ϵ values, respectively, and compare with the reference radius in (7.7). We use a fixed spatial mesh $\Delta x = \Delta y = 2^{-8}$, and consider various time steps of $\Delta t = 0.2560, 0.1280$, and 0.0640. The radius is measured by taking a slice of the solution along $y = 0$, and then solving for $u = 0$ given a linear fit between the two closest points that satisfy $u(x,0,t) < 0$ and $u(x,0,t) > 0$. For each $\epsilon = 0.05$ and $\epsilon = 0.01$, our numerical solutions shrink with the correct velocity. However, given that the reference radius of (7.7) is derived by the assumption that $\epsilon \to 0$, then we expect that the smaller $\epsilon = 0.01$ should be the more accurate than the larger value of $\epsilon = 0.05$. In Figure 4, we directly observe this behavior.

Finally, we demonstrate the order of accuracy of our scheme in two spatial dimensions. First, we extend the second order scheme (7.2) and the third order scheme (7.3) by dimensional splitting method. We use $\epsilon = 0.05$, $\Delta x = \Delta y = 2^{-9}$, and integrate to a final time $T = 0.5$, and again, we use the quadrature method that is fourth order accurate in space for each single-dimensional integral. Given that we do not have an

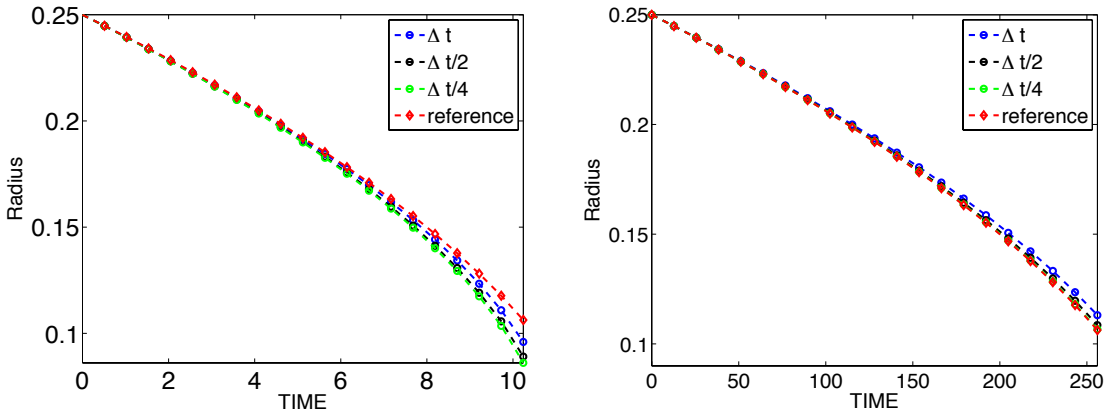

(a) $\epsilon = 0.05$ (b) $\epsilon = 0.01$

Fig. 4: Radii of the interfacial circle as a function of time ($0 \leq t \leq \frac{0.0256}{\epsilon^2}$) compared with the reference radius R (red line) in (7.7).

exact solution, we compute successive errors in an L^∞-norm, that is, we compute $||u_{\Delta t} - u_{\frac{\Delta t}{2}}||_\infty$ for each time step Δt. Results are presented in Table 5. These examples show that our scheme combined with the dimensional splitting obtain the predicted orders of accuracy.

Table 5: Refinement study for a 2D AC equation with a zero Neumann boundary conditions.

	$P=1$		$P=2$		$P=3$	
Δt	L^∞ error	order	L^∞ error	order	L^∞ error	order
0.0063	6.5941×10^{-4}	–	1.1740×10^{-4}	–	5.1744×10^{-6}	–
0.0031	3.3065×10^{-4}	0.9959	3.2637×10^{-5}	1.8468	7.8351×10^{-7}	2.7234
0.0016	1.6563×10^{-4}	0.9973	8.6726×10^{-6}	1.9120	1.0811×10^{-7}	2.8574
0.0008	8.2894×10^{-5}	0.9987	2.2389×10^{-6}	1.9537	1.2961×10^{-8}	3.0602

7.4. Two-dimensional test: The Fitzhugh-Nagumo system. Finally we solve a well-known reaction diffusion system which arises in the modeling of neurons, the Fitzhugh-Nagumo (FHN) model [17, 25]. The FHN system consists of an activator u and an inhibitor v, which are coupled via nonlinear reaction diffusion equations

$$\begin{aligned} u_t &= D_u \nabla^2 u + \frac{1}{\delta} h(u,v), \\ v_t &= D_v \nabla^2 v + g(u,v), \end{aligned} \tag{7.8}$$

where D_u, D_v are the diffusion coefficients for u and v, respectively, and $0 < \delta \ll 1$ is a real parameter. We use the classical cubic FHN local dynamics [25], which are defined as

$$\begin{aligned} h(u,v) &= Cu(1-u)(u-a) - v, \\ g(u,v) &= u - dv, \end{aligned} \tag{7.9}$$

where C, a and d are dimensionless parameters. The parameters we use are the same as in [10, 36]: $D_u = 1$, $D_v = 0$, $a = 0.1$, $C = 1$, $d = 0.5$, and $\delta = 0.005$. The diffusion coefficient for the inhibitor is $D_v = 0$, as considered in [26, 36, 43, 45].

The second order scheme from (7.2) is applied to each variable u and v separately, which defines

$$
\begin{aligned}
u^{n+1} &= e^{\Delta t \nabla^2}\left(u^n + \frac{\Delta t}{2\delta} h^n\right) + \frac{\Delta t}{2\delta} h^{n+1}, \\
v^{n+1} &= \left(v^n + \frac{\Delta t}{2} g^n\right) + \frac{\Delta t}{2} g^{n+1},
\end{aligned} \tag{7.10}
$$

where $h^n = h(u^n, v^n)$ and $g^n = g(u^n, v^n)$. Now, we use the stabilized fixed point iteration to handle the nonlinear term, but it is well-known that $(u^*, v^*) = (0, 0)$ is the only stable excitable fixed point of equation (7.8). To linearize the nonlinear term, we use the Jacobian of $\mathbf{F} = (h, g)$ of (7.9) given by

$$
\mathcal{J}_{\mathbf{F}}(u^*, v^*) \cdot \begin{bmatrix} u - u^* \\ v - v^* \end{bmatrix} \equiv \frac{\partial(h, g)}{\partial(u, v)}|_{(0,0)} \cdot \begin{bmatrix} u \\ v \end{bmatrix} = \begin{bmatrix} -Ca & -1 \\ 1 & -d \end{bmatrix} \begin{bmatrix} u \\ v \end{bmatrix} = \begin{bmatrix} -Cau - v \\ u - dv \end{bmatrix}. \tag{7.11}
$$

With this Jacobian, the simplest fixed point iterative scheme for the second order scheme is

$$
\begin{bmatrix} 1 + \frac{Ca\Delta t}{2\delta} & \frac{\Delta t}{2\delta} \\ -\frac{\Delta t}{2} & 1 + \frac{d\Delta t}{2} \end{bmatrix} \begin{bmatrix} u^{n+1,k+1} \\ v^{n+1,k+1} \end{bmatrix} = \begin{bmatrix} e^{\Delta t \nabla^2}\left(u^n + \frac{\Delta t}{2\delta} h^n\right) \\ v^n + \frac{\Delta t}{2} g^n \end{bmatrix} + \frac{\Delta t}{2} \begin{bmatrix} \frac{1}{\delta}\left(h^{n+1,k} + Cau^{n+1,k} + v^{n+1,k}\right) \\ g^{n+1,k} - u^{n+1,k} + dv^{n+1,k} \end{bmatrix}, \tag{7.12}
$$

where k is the iteration number.

Finally, we consider the domain $\Omega = [-20, 20] \times [-20, 20]$ with periodic boundary conditions and perform temporal integration up to the final times of $T = 1, 2$ and 4. In Figure 5, we present the numerical evolution of the concentration of the activator u from our scheme with the parameters, $\Delta t = 0.001$, and $\Delta x = \Delta y = 0.2$ which shows the same spiral waves that form and can be observed in other recent work from the literature [10].

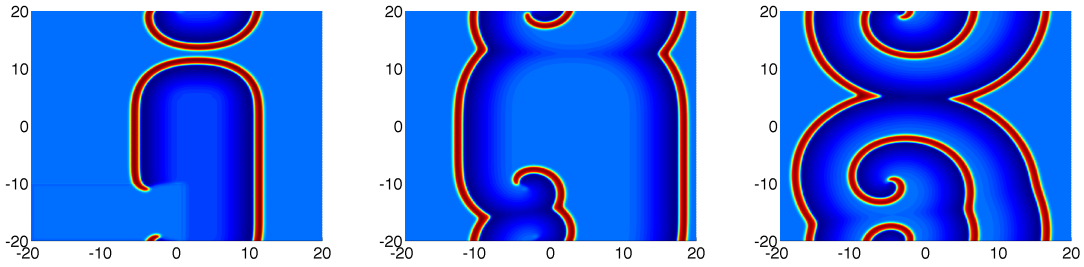

(a) $T = 1$ (b) $T = 2$ (c) $T = 4$

Fig. 5: Temporal evolution of the concentration of activator u from our scheme (7.12).

8. Conclusions. In this work, we have introduced a numerical scheme for parabolic problems, which achieves high order in space and time for the linear heat equation and some sample nonlinear reaction diffusion equations. The scheme is $\mathcal{O}(N)$ for N spatial points, and exhibits stiff decay for any order of accuracy. In the future, we intend to explore parallelization of the algorithm using domain decomposition, which we expect to perform well due to the decoupled spatial factorization that we employ.

REFERENCES

[1] L. Abadias and P. J. Miana. C_0-semigroups and resolvent operators approximated by Laguerre expansions. *arXiv preprint arXiv:1311.7542*, 2013.

[2] S. Allen and J. Cahn. A microscopic theory for antiphase boundary motion and its application to antiphase domain coarsening. *Acta Metallurgica*, 1979.

[3] J. Cahn and J. Hilliard. Spinodal decomposition: A reprise. *Acta Metallurgica*, 19(2):151 – 161, 1971.

[4] J. W. Cahn. On spinodal decomposition. *Acta Metallurgica*, 9(9):795 – 801, 1961.

[5] M. Causley, A. Christlieb, B. Ong, and L. Van Groningen. Method of lines transpose: an implicit solution to the wave equation. *Math. Comp.*, 83(290):2763–2786, 2014.

[6] M. F. Causley and A. J. Christlieb. Higher order A-stable schemes for the wave equation using a successive convolution approach. *SIAM J. Numer. Anal.*, 52(1):220–235, 2014.

[7] M. F. Causley, A. J. Christlieb, Y. Guclu, and E. Wolf. Method of lines transpose: A fast implicit wave propagator. *arXiv preprint arXiv:1306.6902*, 2013.

[8] L. Chen and J. Shen. Applications of semi-implicit Fourier-spectral method to phase field equations. *Computer Physics Communications*, 108(2):147–158, 1998.

[9] A. J. Christlieb, Y. Güçlü, and D. C. Seal. The Picard integral formulation of weighted essentially non-oscillatory schemes. *SIAM J. Numer. Anal.*, 2015. (accepted).

[10] A. J. Christlieb, Y. Liu, and Z. Xu. High order operator splitting methods based on an integral deferred correction framework. *Journal of Computational Physics*, 294:224–242, 2015.

[11] J. Crank and P. Nicolson. A practical method for numerical evaluation of solutions of partial differential equations of the heat-conduction type. *Advances in Computational Mathematics*, 6(3):207–226, 1996.

[12] S. Dai and K. Promislow. Geometric evolution of bilayers under the functionalized Cahn-Hilliard equation. *Proceedings of the Royal Society A: Mathematical, Physical and Engineering Science*, 469(2153), 2013.

[13] J. Douglas, Jr. On the numerical integration of $\frac{\partial^2 u}{\partial x^2} + \frac{\partial^2 u}{\partial y^2} = \frac{\partial u}{\partial t}$ by implicit methods. *Journal of the Society for Industrial and Applied Mathematics*, 3(1):42–65, 1955.

[14] J. Douglas, Jr. Alternating direction methods for three space variables. *Numerische Mathematik*, 4(1):41–63, 1962.

[15] J. Douglas, Jr. and H. Rachford. On the numerical solution of heat conduction problems in two and three space variables. *Transactions of the American mathematical Society*, 82(2):421–439, 1956.

[16] G. Fairweather and A. Mitchell. A new computational procedure for ADI methods. *SIAM Journal on Numerical Analysis*, 4(2), 1967.

[17] P. C. Fife et al. *Mathematical aspects of reacting and diffusing systems.* Springer Verlag., 1979.

[18] R. A. Fisher. *The genetical theory of natural selection: a complete variorum edition.* Oxford University Press, 1999.

[19] R. FitzHugh. Impulses and physiological states in theoretical models of nerve membrane. *Biophysical journal*, 1(6):445–466, 1961.

[20] L. Greengard and J. Strain. The fast Gauss transform. *SIAM J. Sci. Statist. Comput.*, 12(1):79–94, 1991.

[21] V. Grimm and M. Gugat. Approximation of semigroups and related operator functions by resolvent series. *SIAM Journal on Numerical Analysis*, 48(5):1826–1845, 2010.

[22] J. Jia and J. Huang. Krylov deferred correction accelerated method of lines transpose for parabolic problems. *Journal of Computational Physics*, 227(3):1739–1753, Jan. 2008.

[23] S. Jiang, L. Greengard, and S. Wang. Efficient sum-of-exponentials approximations for the heat kernel and their applications. *arXiv preprint arXiv:1308.3883*, pages 1–23, 2013.

[24] A. Kassam and L. Trefethen. Fourth-order time-stepping for stiff PDEs. *SIAM Journal on Scientific Computing*, 26(4):1214–1233, 2005.

[25] J. P. Keener and J. Sneyd. *Mathematical physiology*, volume 1. Springer, 1998.

[26] V. Krinsky and A. Pumir. Models of defibrillation of cardiac tissue. *Chaos: An Interdisciplinary Journal of Nonlinear Science*, 8(1):188–203, 1998.

[27] M. C. A. Kropinski and B. D. Quaife. Fast integral equation methods for the modified Helmholtz equation. *J. Comput. Phys.*, 230(2):425–434, 2011.

[28] J. V. Lambers. Implicitly defined high-order operator splittings for parabolic and hyperbolic variable-coefficient PDE using modified moments. *Int. J. Pure Appl. Math.*, 50(2):239–244, 2009.

[29] H. G. Lee and J.-Y. Lee. A semi-analytical Fourier spectral method for the Allen-Cahn equation. *Comput. Math. Appl.*, 68(3):174–184, 2014.

[30] J. Li and L. Greengard. High order accurate methods for the evaluation of layer heat potentials. *SIAM Journal on Scientific Computing*, 31(5):3847–3860, 2009.

[31] C. Lubich and R. Schneider. Time discretization of parabolic boundary integral equations. *Numerische Mathematik*, 455481, 1992.

[32] M. Lyon and O. Bruno. High-order unconditionally stable FC-AD solvers for general smooth domains II. Elliptic, parabolic and hyperbolic PDEs; theoretical considerations. *Journal of Computational Physics*, 229(9):3358–3381, 2010.

[33] M. Lyon and O. P. Bruno. High-order unconditionally stable FC-AD solvers for general smooth domains. II. Elliptic, parabolic and hyperbolic PDEs; theoretical considerations. *J. Comput. Phys.*, 229(9):3358–3381, 2010.

[34] J. Nagumo, S. Arimoto, and S. Yoshizawa. An active pulse transmission line simulating nerve axon. *Proceedings of the IRE*, 50(10):2061–2070, 1962.

[35] S. P. Nørsett. One-step methods of Hermite type for numerical integration of stiff systems. *BIT Numerical Mathematics*, 14, 1974.

[36] D. Olmos and B. D. Shizgal. Pseudospectral method of solution of the Fitzhugh-Nagumo equation. *Math. Comput. Simulation*, 79(7):2258–2278, 2009.

[37] D. W. Peaceman and H. H. Rachford, Jr. The numerical solution of parabolic and elliptic differential equations. *J. Soc. Indust. Appl. Math.*, 3:28–41, 1955.

[38] E. Rothe. Zweidimensionale parabolische Randwertaufgaben als Grenzfall eindimensionaler Randwertaufgaben. *Math. Ann.*, 102(1):650–670, 1930.

[39] A. J. Salazar, M. Raydan, and A. Campo. Theoretical analysis of the exponential transversal method of lines for the

diffusion equation. *Numer. Methods Partial Differential Equations*, 16(1):30–41, 2000.
[40] D. C. Seal, Y. Güçlü, and A. J. Christlieb. High-order multiderivative time integrators for hyperbolic conservation laws. *Journal of Scientific Computing*, 60(1):101–140, 2014.
[41] J. Shen and X. Yang. Numerical approximations of Allen-Cahn and Cahn-Hilliard equations. *Discrete Contin. Dyn. Syst.*, 28(4):1669–1691, 2010.
[42] S. Shreve. *Stochastic Calculus for Finance II: Continuous-Time Models*. Number v. 11 in Springer Finance. Springer, 2004.
[43] J. Starobin and C. Starmer. Common mechanism links spiral wave meandering and wave-front–obstacle separation. *Physical Review E*, 55(1):1193, 1997.
[44] J. Tausch. A fast method for solving the heat equation by layer potentials. *Journal of Computational Physics*, 224(2):956–969, June 2007.
[45] F. Xie, Z. Qu, J. N. Weiss, and A. Garfinkel. Coexistence of multiple spiral waves with independent frequencies in a heterogeneous excitable medium. *Physical Review E*, 63(3):031905, 2001.